Desalination and Water Treatment
www.deswater.com

doi: 10.1080/19443994.2014.966277

56 (2015) 3054–3066
December

Taylor & Francis
Taylor & Francis Group

Effect of co-existing ions on electrode behavior in electrocoagulation process for silica removal

Suli Zhi, Shuting Zhang*

School of Environmental Science and Engineering, Tianjin University, Tianjin 300072, China, Tel. +86 13752562238; email: zhisuli87@163.com (S. Zhi), Tel. +86 22 87402148; email: zhangst8740@163.com (S. Zhang)

Received 27 February 2014; Accepted 6 September 2014

ABSTRACT

A continuous electrocoagulation system with two aluminum electrodes was established to remove silica. The mechanism of voltage rise and the effect of anions on electrode behavior were explored in a long-time operation. The ratios of equivalent resistance variation ($\Delta r_c/\Delta r_a$) were 1.76, 5.41, and 8.48% at pH 6.0, 7.0, and 9.0, respectively, which indicated that the voltage rise was mainly controlled by anodic overpotential. The study on anions effect showed that Cl^- could effectively prevent the voltage rise, but it could form disinfection by-products. $[NO_3^-]/[SO_4^{2-}] = 0.1$ was the best ratio for delaying the voltage rise, which means it can be used as the most favorable supporting electrolyte in silica removal by electrocoagulation. Furthermore, cations type had no effect on the voltage rise. Central composite design under response surface methodology was used to optimize the continuous process. The optimal conditions are current density 144.06 A/m^2, retention time 25.95 s, and pH value 7.29, resulting in silica concentrations in the treated effluent below 5 mg/L.

Keywords: Electrocoagulation; Aluminum electrode; Voltage; Resistance; Response surface methodology

1. Introduction

Recently, a large amount of fresh water, about 70% of water for industrial use, is used as cooling water for its high heat capacity and cost-effectiveness [1], which aggravates the shortage of water. However, cooling water recycling can lead to ions concentrating to a critical point for the evaporation of water, which usually result in scaling [2]. Silica scale is a big technical challenge and a big financial burden for industrial operators. It has the smallest thermal conductivity of all scales, about 1/240–1/124 of that of steel. American Electric Power Research Institute reported that 70% of water in power plants was limited by the concentration of silica. This kind of scale can reduce boiler power output by 10–20% and thermal efficiency by 10% [3], plug the pipeline [4], and make more shutdowns [2]. Thus, the potential hazard of silica must come into notice, and more studies should be made to remove silica to recycle cooling water.

Comparing with chemical flocculation, electrocoagulation needs no large amounts of chemicals, has a small precipitate production, is eco-friendly, and easy to operate [5,6]. And some studies have reported that it could be used to remove silica from cooling water. Gelover-Santiago et al. [7] tested three electrochemical

---

*Corresponding author.

systems for treatment of cooling water, and the most advantageous system was the one with both aluminum electrodes working with direct current. Liao et al. [8] investigated the effectiveness of electrocoagulation using iron and aluminum electrodes for treating cooling tower blowdown waters containing dissolved silica, Ca^{2+}, and Mg^{2+}, which concluded that aluminum electrode was more effective for silica removal than iron electrode. Schulz et al. [9] pointed out that the pilot electrocoagulation process with aluminum electrodes underperformed the bench unit due to fouling on aluminum surfaces after few hours of operation when treating cooling water by electrocoagulation process. In addition, electrocoagulation process was also reported to remove silica from brackish water [10] and polishing wastewater [11–13]. Overall, the existing studies show that aluminum electrode is more favorable for silica removal, but it is likely to be passivated in a long-time operation.

Some researchers have reported the effect of anions on the performance of electrocoagulation process with aluminum electrodes [14–18]. Consistent conclusion is that Cl^- can effectively break the passivation layer on aluminum surface and SO_4^{2-} aggravates the passivation of aluminum electrodes. Nevertheless, the interaction of anions is controversial [19]. Up to now, most of the experimental results were obtained in a batch reactor for a short-time operation. However, the effect of anions in a long-time operation is more significant for industrial application.

In the present work, a continuous electrocoagulation process was established to study the effect of co-existing ions on the behavior of aluminum electrodes. Response surface methodology (RSM) [20], which is time saving and reduces workloads, was used to optimize the operating conditions. The following works are discussed: (1) determining the main reason of electrodes passivation by analyzing the equivalent resistances; (2) investigating the effect of different co-existing ions; (3) establishing the prediction model of the continuous process to remove silica.

2. Materials and methods

2.1. Equipment

The experimental setup made of plexiglass is shown in Fig. 1. The artificial wastewater containing silica was pumped from feed water tank, circulated through the electrochemical cell, and flowed into the effluent water tank. Aluminum electrodes were used in the electrochemical cell and the operating parameters are shown in Table 1.

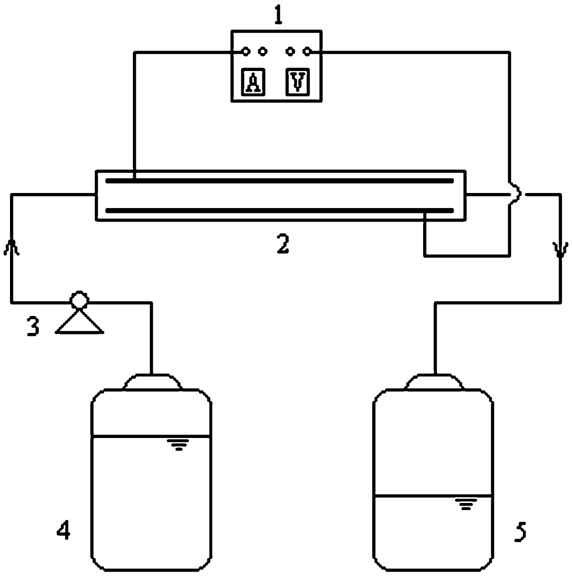

Fig. 1. Schematic diagram of experimental setup 1 digital DC power supply, 2 electrochemical cell, 3 pump, 4 feed water tank, and 5 effluent water tank.

Table 1
Operating parameters of electrochemical cell

Parameter	Unit	Setting value
Electrode spacing	mm	4
Number of electrode	Piece	2
Effective area	cm^2	50 (*L*) × 2 (*W*)
Volume of cell	L	0.04
Feed water flow	L/min	0.24, 0.12, 0.10, 0.08
Residence time of water	s	10, 20, 25, 30

2.2. Methods

The artificial wastewater of cooling water with a silica concentration of 60 mg/L was prepared by dissolving $Na_2SiO_3 \cdot 9H_2O$ in running water. Reagents used in the experiments were all analytical grade.

Table 2 shows the various experimental runs carried out in this work. The objective of run 1 is to investigate the electrode passivation which is represented by the rise of the applied voltage under different current densities, after a long-time operation for silica removal. Run 2 aims to investigate the effect of different anions on the behavior of aluminum electrodes. And the co-effect of the anions is studied as shown in run 3. The type of cations affecting the electrode surface is explored in run 4.

DC power supply (DH1718E-6, Beijing) runs for 1 h to ensure the stability of instrument. Each experimental run was conducted with new electrodes. Electrodes

Table 2
Experimental runs for investigation

Run	Fixed parameters	Setting conditions
1	pH 8.0 Q = 0.24 L/min	SiO_2 (60 mg/L) + J = 50 A/m^2 SiO_2 (60 mg/L) + J = 100 A/m^2 SiO_2 (60 mg/L) + J = 200 A/m^2
2	pH 8.0 J = 100 A/m^2 Q = 0.12 L/min	SiO_2 (60 mg/L) + NaCl + HCl SiO_2 (60 mg/L) + $NaNO_3$ + HNO_3 SiO_2 (60 mg/L) + Na_2SO_4 + H_2SO_4
3	pH 8.0 J = 100 A/m^2 Q = 0.12 L/min	SiO_2 (60 mg/L) + $[Cl^-]/[SO_4^{2-}]$ SiO_2 (60 mg/L) + $[Cl^-]/[NO_3^-]$ SiO_2 (60 mg/L) + $[NO_3^-]/[SO_4^{2-}]$
4	No pH adjustment J = 100 A/m^2 Q = 0.24 L/min	SiO_2 (60 mg/L) + NaCl (1.64 mmol/L) SiO_2 (60 mg/L) + HCl (1.64 mmol/L) SiO_2 (60 mg/L) + NaCl (2.58 mmol/L) SiO_2 (60 mg/L) + HCl (2.58 mmol/L) SiO_2 (60 mg/L) + NaCl (4.22 mmol/L) SiO_2 (60 mg/L) + HCl (4.22 mmol/L)

replacement was adopted in some experimental runs to ensure that one of the electrodes was studied while other conditions were kept constant.

3. Results and discussion

3.1. The behavior of electrode under different current densities

In a continuous electrocoagulation process of silica removal, electrode inactivation can result in the rise of voltage when current density is constant. This paper focuses on the rise of voltage under constant current density, as shown in Fig. 2. When the current densities are given, the applied voltage has a slight decrease in the first 5 h, followed by a stable stage, then a sudden rise at a certain point.

When aluminum electrode is used, aluminum oxidation results in the formation of Al^{3+}, which hydrolyzes to form hydroxides depending on the pH [21].

At the anode:

$$Al_{(s)} \rightarrow Al^{3+} + 3e^- \tag{1}$$

$$Al^{3+} + nH_2O \rightarrow Al(OH)_n^{3-n} + nH^+ \tag{2}$$

Side reaction:

$$4OH^- - 4e^- \rightarrow 2H_2O + O_2 \uparrow \tag{3}$$

At the cathode:

$$6H_2O + 6e^- \rightarrow 3H_2 + 6OH^- \tag{4}$$

Freshly formed amorphous “sweep flocs” can remove various pollutants for its large surface areas. Then, $Al(OH)_n^{3-n}$ [22] reacts with dissolved silica forming

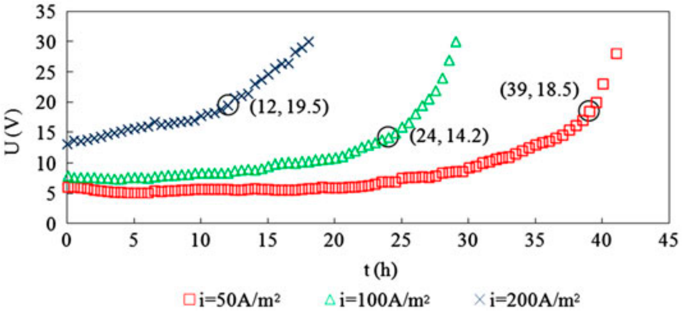

Fig. 2. Change of applied voltage under different current densities.

$(\mathrm{AlO})_n(\mathrm{SiO})_{n/2}(\mathrm{OH})_{2n}$ [10] to purify silica-containing wastewater.

The rise of voltage may be explained by cathodic and anodic passivation reported as follows:

In the microenvironment of cathode, the aluminum ions are very likely to form deposits on the electrode surface causing passivation, physical obstruction on the surface, and increased the power consumption [23]. It is generally accepted that a chemisorbed hydroxide film is formed initially as follows:

$$\mathrm{Al} + \mathrm{H_2O} \rightarrow \mathrm{AlOH} + \mathrm{H^+} + \mathrm{e^-} \tag{5}$$

AlOH either reacts with a water molecule as follows, causing the passivation of the metal:

$$\mathrm{AlOH} + \mathrm{H_2O} \rightarrow \mathrm{AlOOH} + \mathrm{H_2} \tag{6}$$

or undergoes dissolution reactions as follows:

$$\mathrm{AlOH} + \mathrm{OH^-} \rightarrow \mathrm{AlO_2^-} + \mathrm{H_2} \tag{7}$$

The passive oxide film on aluminum anode may exist due to oxygen generated [24], which is not electron conducting and results in high anodic dissolution overpotential [25] and some chemisorbed hydroxide film also can be adsorbed on the anode.

In our experiment, although film growth and chemical or electrochemical dissolution took place simultaneously during the electrode polarization of aluminum, the applied voltage went up after a long-time operation (as shown in Fig. 2), which resulted in the high power consumption. The electrodes continually clogged up, long before the metal had been adequately sacrificed into solution, which meant that the metal electrodes must be replaced at a high cost, making the process uneconomic.

In the first 5 h, aluminum oxidation reaction made the surface of anode plate rough from flat surface, which increased the effective area of electrode resulting in a slight drop of voltage.

Moreover, in Fig. 2, there are turning points in the curves of the applied voltage with time, after which the voltage increases more drastically. When current densities are 50, 100, and 200 $\mathrm{A/m^2}$, the turning points are (39, 18.5), (24, 14.2), and (12, 19.5), respectively; where, the charges that have passed through the electric circuit are 70,200, 86,400, and 86,400 C, respectively. It is an interesting conclusion that the electric quantities are accumulated to a similar level under different conditions, when the voltage begins to rise suddenly. This means that electrocoagulation process can use a predetermined amount of charge as an indication of the degree to which the electrodes are replaced, and allows for greater flexibility in application.

3.2. Electrical resistance during electrocoagulation process

In order to determine the main reason for the rise of applied voltage, the potentials and equivalent resistances of the electrocoagulation cell were analyzed.

Eq. (8) expresses the applied voltage in the electrocoagulation cell:

$$E_{\mathrm{AP}} = E_{\mathrm{s}} + E_{\mathrm{a}} + E_{\mathrm{c}} + \eta_{\mathrm{a}} + \eta_{\mathrm{c}} \tag{8}$$

The term E_{a} is the potential of evolution reaction on the surface of the anode, determined by the kinetics of the electrochemical reaction. η_{a} is the overpotential due to passivation of the anode, E_{c} is the potential of evolution reaction on the surface of the cathode, η_{c} is the overpotential due to passivation of the cathode, and E_{s} is the potential drop of solution determined by Ohm's law:

$$E_{\mathrm{s}} = Id/Ak \tag{9}$$

The current (I), the distance between each electrode (d), and the active electrode area (A) were maintained constant in all experiment runs. Table 3 presents the initial and final conductivity in different solutions; they were almost the same. Accordingly, E_{s} in each solution can be regarded as constant. Thus, the overpotential can be determined by Eq. (10):

$$\eta = E_{\mathrm{AP}} - E_{\mathrm{a}} - E_{\mathrm{c}} - E_{\mathrm{s}} \tag{10}$$

Table 3
Comparison of conductivities of different solutions

Parameter	Influent conductivity (μs/cm)	Effluent conductivity (μs/cm)
No additive	909.6 ± 5.4	872.2 ± 5.1
NaCl	1,077.8 ± 18.7	1,042.6 ± 16.0
$\mathrm{NaNO_3}$	1,039.8 ± 15.3	998.8 ± 10.6
$\mathrm{Na_2SO_4}$	1,142.1 ± 9.2	1,103.7 ± 8.4

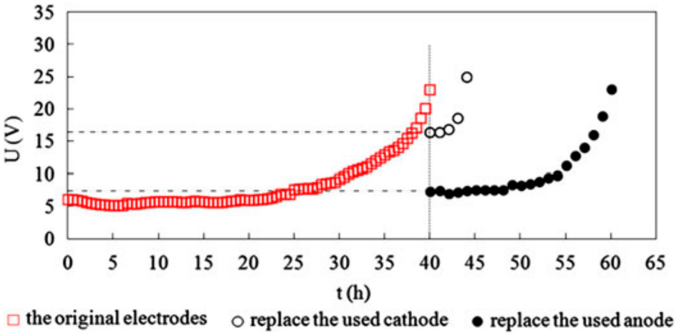

Fig. 3. Change of voltage with time under constant current density.

Fig. 3 shows the change of the applied voltage with time. When the reaction time was 40 h, one of the two used electrodes was replaced by a new one. It can be seen that when the used cathode was replaced by a new one, the voltage reduced to 16.5 V from 23.0 V, and then increased to 23.0 V in 4 h. While the used anode was replaced by a new one, the voltage immediately dropped to 7.0 V, and then reached 23.0 V in 20 h. Hence, it seems that the change of the anode overpotential controls the whole applied voltage.

When the current is constant, the change of applied voltage is controlled by the resistance according to the Ohm's law. To determine the oxide film resistance on the surface of electrodes, the electric equivalent circuit is given in Fig. 4.

In the circuit, the overall resistance can be expressed by Eq. (11):

$$R_{\text{overall}} = R_a + r_a + R_s + r_c + R_c \tag{11}$$

where R_a and R_c are the equivalent resistances for E_a and E_c, respectively. r_a and r_c are the equivalent resistances due to the passivation of anode and cathode surface (for η_a and η_c), respectively. R_s is the equivalent resistance of electrolyte (for E_s). In this given electrocoagulation system, R_a, R_c, and R_s are not variational in each experiment run when current density, electrode materials, and electrolyte are fixed. Therefore, r_a and r_c are mainly considered as below.

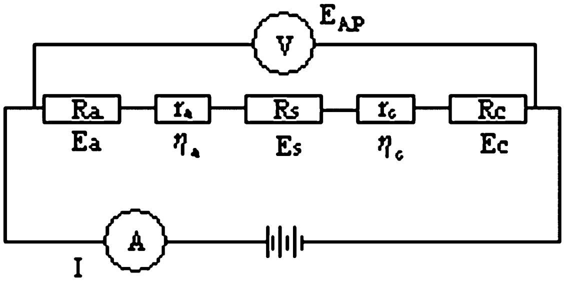

Fig. 4. Electric equivalent circuit of electrochemical cell.

Evaluation of r_a and r_c is based on the comparison of the equivalent resistances under different conditions.

Fig. 5 shows the changes of voltage with current under different pH values. Here, r_{a0} and r_{c0} are respectively, the initial partial coverage resistance (the initial oxide film on the surface of new electrodes) of a couple of new electrodes, and they can be assumed to be zero. Then,

$$\Delta r_a = r_a - r_{a0} \tag{12}$$

$$\Delta r_c = r_c - r_{c0} \tag{13}$$

where Δr_a and Δr_c stand for the resistance changes due to the passivation of anode and cathode surface, respectively, during electrocoagulation.

When one of the two used electrodes was replaced, for example the used cathode, the total resistance change of the whole electrochemical cell represented the anodic resistance change. Therefore, the following equations are proposed:

$$\Delta r_a = r_a^B - r_a^A = R_{\text{overall}}^B - R_{\text{overall}}^A \tag{14}$$

$$\Delta r_c = r_c^B - r_c^A = R_{\text{overall}}^B - R_{\text{overall}}^A \tag{15}$$

where the superscript A and B represent "After the replacement" and "Before the replacement."

From the diagrams of U-I (Fig. 5), we can conclude the value of ($R_{\text{overall}}^B - R_{\text{overall}}^A$) according to the slope of lines under different pH values. Then, Δr_a and Δr_c are obtained, and $\Delta r_c/\Delta r_a$ ratios obtained are 1.76, 5.41,

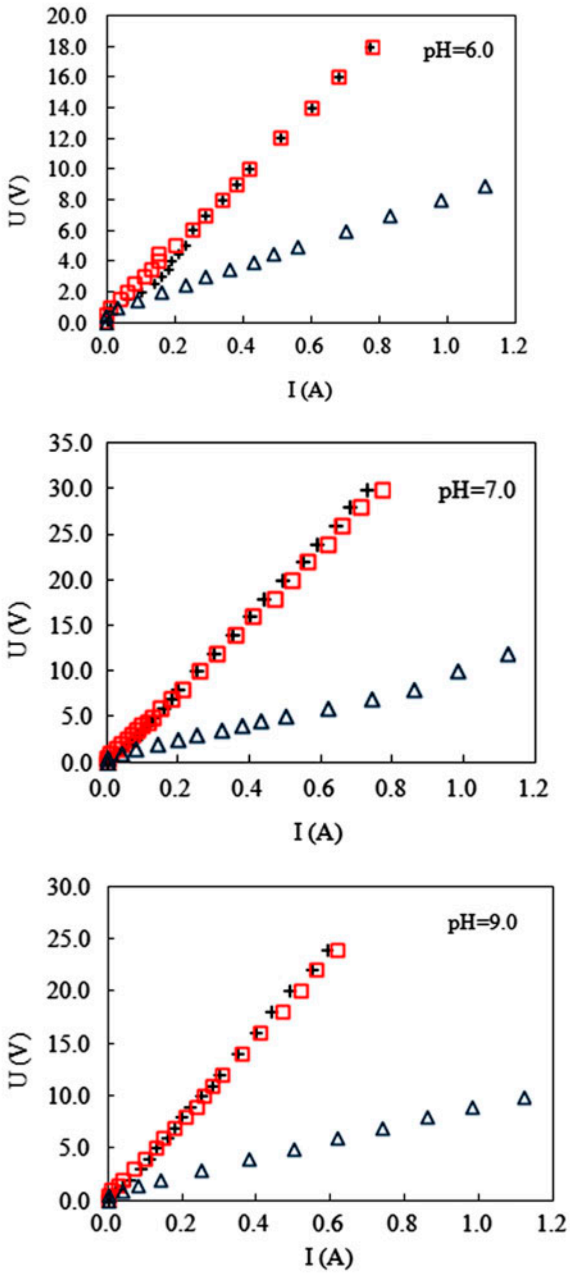

Fig. 5. Change of voltages with current under different pH values: □ new cathode and used anode; Δ new anode and used cathode; + used anode and used cathode.

and 8.48%, respectively, at pH 6.0, 7.0, and 9.0, which clearly illustrated that the increase of resistance in the circuit is mainly caused by the anode resistance due to passivation. Besides, the ratio of $\Delta r_c/\Delta r_a$ increases with the increase of initial pH values, which reveals that the passivation on cathode surface is more serious in alkaline conditions. This can be explained by Eqs. (5) and (6) as mentioned above.

3.3. Effect of anions

3.3.1. Separate effect of anions

Since the anode passivation has a more significant impact on the voltage rise, the effects of different anions (Cl^-, NO_3^-, and SO_4^{2-}) on the voltage rise were considered to investigate the behavior of aluminum electrode. In order to study the separate effect of Cl^-, NO_3^-, and SO_4^{2-}, different concentrations of anions and their corresponding acids were added in electrolyte (run 2 in Table 2). The results are shown in Fig. 6. Fig. 6 shows the variation of voltage with electrolytic time under different Cl^- concentrations. It is concluded that the higher concentration of Cl^- contributes more to prevent the rise of applied voltage. When Cl^- concentrations are 1.8, 3, and 4 mmol/L, the turning points in the curves of the applied voltage are (24, 14.2), (29, 15.7), and (33, 15.6), respectively. However, the availability of Cl^- in the water can cause formation of disinfection by-products (DBPs) which are suspected carcinogenic compounds [26]; so, adding Cl^- to water must be avoided.

It is generally accepted that chloride ion is much smaller one and has a stronger penetrating ability. Many authors [27–29] have reported that Cl^- could change the composition of oxide film on the aluminum surface due to Cl^- incorporation into the film in the pre-pitting stage below the pitting potential.

Lee and Pyun [30] analyzed the aggressive chlorine ion, which corrodes Al electrode by pitting corrosion as follows:

$$Al(OH)_3 + Cl^- = Al(OH)_2Cl + OH^- \tag{16}$$

$$Al(OH)_2Cl + Cl^- = Al(OH)Cl_2 + OH^- \tag{17}$$

$$Al(OH)Cl_2 + Cl^- = AlCl_3 + OH^- \tag{18}$$

$$AlCl_3 + Cl^- = AlCl_4^- \tag{19}$$

Such transitory compounds like $Al(OH)_2Cl$, $AlOHCl_2$, and $AlCl_3$, which can be dissolved chemically as $AlCl_4^-$ above the pitting potential, thereby resulting in pit ignition, can maintain the dissolution of aluminum. This is why Cl^- can effectively prevent the rise of voltage.

Fig. 7 shows the variation of voltage with electrolytic time under different NO_3^- concentrations. Though higher concentration of NO_3^- leads to later rise of voltage, the effect of NO_3^- is not obvious. About nitrate as supporting electrolyte, different conclusions were reported. Generally, NO_3^- present in water nearly has no effect on electrocoagulation process [19]. Amani-Ghadim et al. [18] commented that electrocoagulation performance

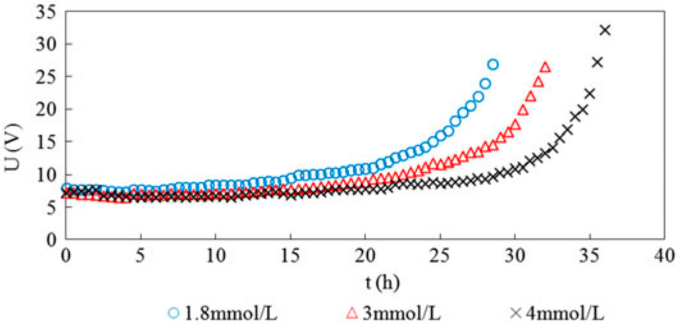

Fig. 6. The variation of voltage with electrolytic time under different Cl^- concentrations.

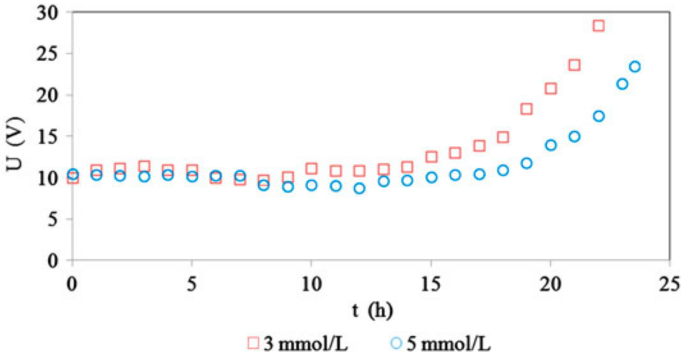

Fig. 7. The variation of voltage with electrolytic time under different NO_3^- concentrations.

declined greatly when nitrate was added, but dissolved the amount of aluminum which was almost as same as that of solution with Cl^-. According to Hu et al. [24], NO_3^- is an anion which prevented the inhibition of SO_4^{2-}. In our experiment, the effect of NO_3^- on the voltage rise depended on its concentration and the relations with other anions, which will be analyzed in the following part of this paper.

Fig. 8 shows the variation of voltage with electrolytic time under different SO_4^{2-} concentrations. Obviously, SO_4^{2-} accelerates the voltage rise and this acceleration is enhanced by the increase in SO_4^{2-} concentration. Just as reported, SO_4^{2-} has a negative effect on electrocoagulation process [24]. Some studies pointed out that Cl^- and NO_3^- incorporate into the oxide on pure Al, whereas sulfate ions (SO_4^{2-}) just adsorbs on the oxide film [30] and delays pit initiation on the outer oxide-covered surface of pure Al, owing to their competitive adsorption with Cl^-. Foley and Nguyen [31] measured the energy levels of the transitory compounds, and showed that the intermediate specie $Al(OH)SO_4$ has a lower energy than $Al(OH)_3$. This is why SO_4^{2-} ion accelerated the rise of voltage.

Through comparing the turning points in the curves of different anions, it can be concluded that the point-in-time for sudden rise of voltage are 29 h, 18 h, and 14 h for Cl^-, NO_3^-, and SO_4^{2-} (3 mmol/L), respectively. It illustrates that Cl^- is the most effective one to prevent voltage rise, but its availability has potential risk. NO_3^- has no remarkable effect and SO_4^{2-} has negative effect. Therefore, it is necessary to find a favorable supporting electrolyte which has excellent effect on the behavior of aluminum electrode.

3.3.2. Co-effect of anions

Considering the complexity of water, the relations of different anions were studied. Fig. 9 shows the effect of $[Cl^-]/[SO_4^{2-}]$ ratio on the rise of voltage. It can be seen that with the increasing $[Cl^-]/[SO_4^{2-}]$ ratio, the rise of voltage occurs much later. It was reported that the corrosive power of Cl^- was predominant when $[Cl^-]/[SO_4^{2-}]$ ratio was around or >0.1 [16]. Although SO_4^{2-} can deteriorate the electrode passivation, it can be overcome by adding little amount of Cl^-. In our study, when $[Cl^-]/[SO_4^{2-}]$ ratio was smaller

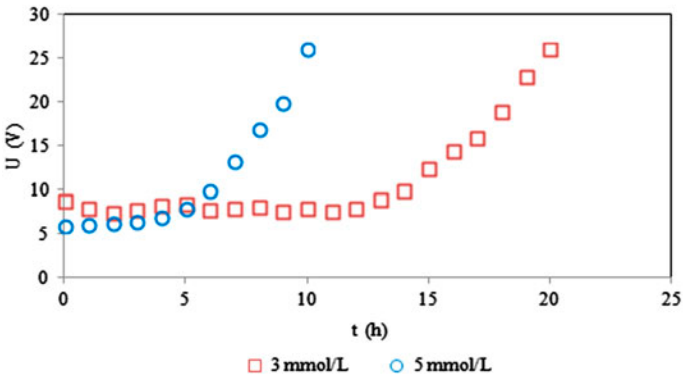

Fig. 8. The variation of voltage with electrolytic time under different SO_4^{2-} concentrations.

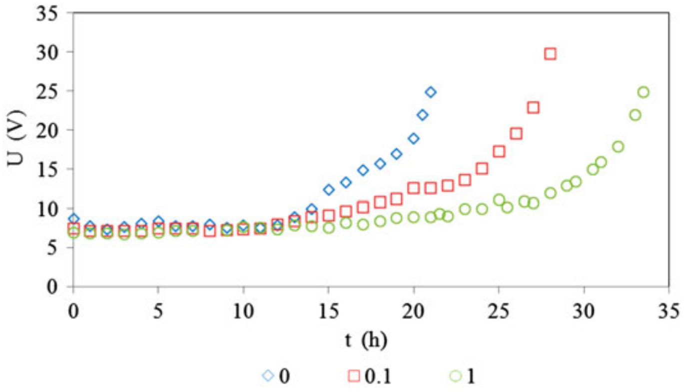

Fig. 9. The effect of $[Cl^-]/[SO_4^{2-}]$ ratio on the rise of voltage.

than 0.1, the electrode reaction could still proceed which was mainly due to the complexity of water.

Fig. 10 shows the effect of $[Cl^-]/[NO_3^-]$ ratio on the rise of voltage. When the ratio increases to 0.1 from 0, the rise of voltage is prevented considerably much by 4.5 h. When the ratio increases to 1 from 0.1, the rise of voltage is prevented only by 1.5 h. This shows that increasing $[Cl^-]/[NO_3^-]$ ratio >0.1 has no matching contribution.

Fig. 11 shows the effect of $[NO_3^-]/[SO_4^{2-}]$ ratio on the rise of voltage. We can see that the latest rise of voltage occurs at $[NO_3^-]/[SO_4^{2-}] = 0.1$. However, when adding more NO_3^- ($[NO_3^-]/[SO_4^{2-}] = 1$), the rise of voltage is accelerated. This may be because the large amount of NO_3^- and SO_4^{2-} results in severe oxidation of aluminum electrode. Therefore, $[NO_3^-]/[SO_4^{2-}] = 0.1$ is the best ratio for silica removal by electrocoagulation.

Since adding Cl^- results in the formation of DBPs, the electrolyte with $[NO_3^-]/[SO_4^{2-}] = 0.1$ can be used as a supporting electrolyte for electrocoagulation process to remove silica.

3.4. *Effect of cations*

Solutions with same amount but different type of cations were prepared to explore how the type of univalent cations affects the applied voltage. Fig. 12 shows the variations of applied voltage of solutions with HCl and NaCl. When the amount of Cl^- is fixed, the voltage evolution plot is similar whether the Cl^- provided by HCl or NaCl. Table 4 presents pH values of different solutions. The solutions with same amount of Cl^- but different type of cations have very different pH values. It seems that the pH value has little effect on the rise of applied voltage, when the concentrations of Cl^- are same.

The pH value is one of the important factors affecting the performance of electrochemical process [32]. It controls the dissolution reaction of aluminum and its hydroxides, thereby affecting the removal process. Fig. 13 shows the evolution of pH values for treated solution of different initial pH values. Obviously, electrocoagulation system can work as pH neutralization, just as reported in other works [33]. A pH

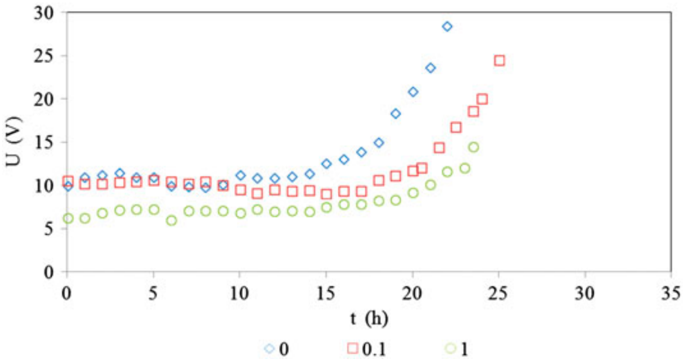

Fig. 10. The effect of $[Cl^-]/[NO_3^-]$ ratio on the rise of voltage.

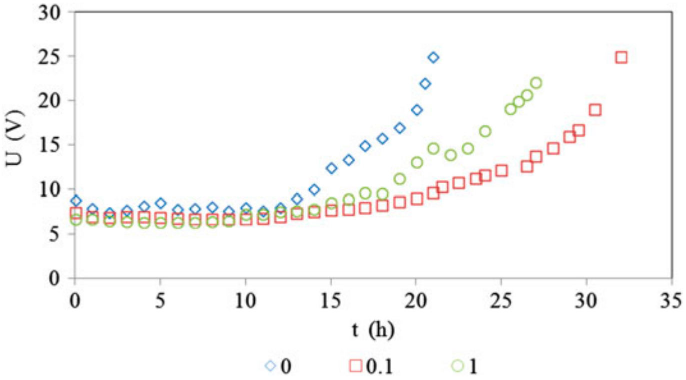

Fig. 11. The effect of $[NO_3^-]/[SO_4^{2-}]$ ratio on the rise of voltage.

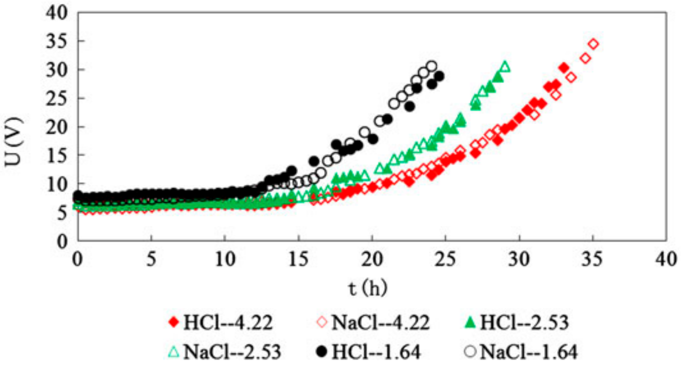

Fig. 12. Effect of NaCl and HCl on the rise of applied voltage.

Table 4
Initial pH values of different solutions

	1.64 mmol/L		2.58 mmol/L		4.22 mmol/L	
C_{Cl^-}	+HCl	+NaCl	+HCl	+NaCl	+HCl	+NaCl
pH	8.62	9.98	6.66	9.94	4.95	9.90

increase occurs when the initial pH is acidic, and a pH drop occurs when the initial pH is alkaline. However, in highly alkaline electrolyte (pH_i 10), the system is not sufficient to decrease the pH of the solution to neutral. This was because the residence time of electrolyte (10 s) was too short to adjust the pH of effluent.

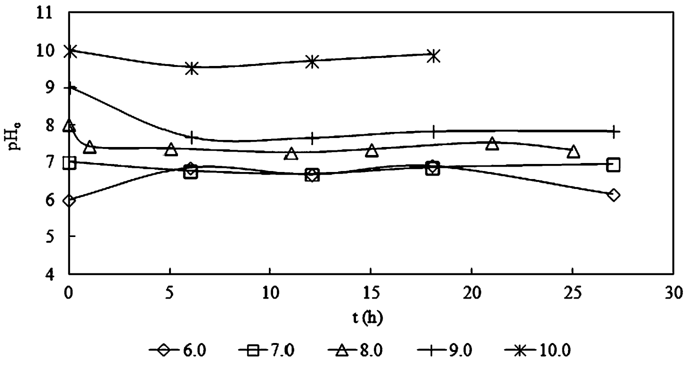

Fig. 13. Change of effluent pH values of different solutions under different initial pH values.

3.5. Features of electrode surface

For illuminating that the anode overpotential controls the whole voltage, the photograph of electrodes is shown in Fig. 14. We can see that the amount of sediment on the electrodes is considerably macroscopic after a long-time operation. The sediment on anode surface is much more than that on cathode surface. It is widely proved that aluminum cathode is attacked by OH^- produced on cathode surface for water reaction (4). Then, sediment of aluminum hydroxide will form on the cathode surface. However, Al^{3+} produces from anode surface when electric current is applied. And it immediately hydrolyzes to yield flocculants in the boundary layer near the anode surface. Moreover, silicate which is usually negatively charged migrates to the anode surface. Therefore, the products of aluminum hydroxide and silicate forms near the anode surface. The floc of aluminum hydroxide and silicate is negatively charged according to our results (data not shown), which indicates that the floc may adsorb to the anode surface. This is the reason for abundant sediment on the anode surface.

3.6. Optimization of silica removing

RSM is a collection of mathematical and statistical techniques that is useful for analyzing the effects of several independent variables on the response. Central composite design (CCD) is most frequently applied under RSM design [34]. In this study, CCD was used to optimize the silica removal by studying the effect of three independent variables including current density, retention time, and pH value on the response of effluent silica concentration with the coded values at three levels (−1, 0, and +1). Therefore, the ranges of the independent variables are current density (x_1: 50–100 A/m^2), retention time (x_2: 20–30 s), and pH value (x_3: 5–10).

Table 5 shows regression coefficients, and corresponding F and p values for effluent silica concentration. Values of "Prob > F" less than 0.0500 indicate model terms are significant. In the case, x_1, x_2, x_3, and x_1^2 are significant model terms. By applying regression analysis, the empirical relationship between effluent silica concentration Y (mg/L) and the three variables in coded units was given by:

$$Y = 10.58 - 8.78x_1 - 1.96x_2 - 10.66x_3 - 1.17x_1x_2 + 1.75x_1x_3 - 1.95x_2x_3 + 2.47x_1^2 + 0.32x_2^2 + 1.17x_3^2 \quad (20)$$

Table 6 shows the ANOVA results of the model for effluent silica concentration. The model F value is 108.51 and Prob > F is less than 0.0001, which implies the model is significant. The fit of the model was checked by the adjusted determination coefficient (adjR^2). In the study, adjR^2 = 0.9857 indicates that the model predicts the response better. The coefficient of variance (CV) as the ratio of the standard error of estimate to the mean value of the observed response is a measure of reproducibility of the model. As shown in Table 6, the value of CV is 8.45%. "Adeq Precision" (AP) measures the signal to noise ratio. A ratio >4 is desirable. The ratio of 39.901 indicates an adequate signal. This model can be used to navigate the design space.

For the graphical interpretation of the interactions, the contour plots describing the tendency of effluent silica concentration with respect to current density, retention time, and pH value are shown in Fig. 15. As it can be seen, the effluent silica concentration decreased with increasing current density, retention time, and pH value. The higher current density would result in more dissolved Al^{3+} from anode surface, which could combine more silica in definite time. The

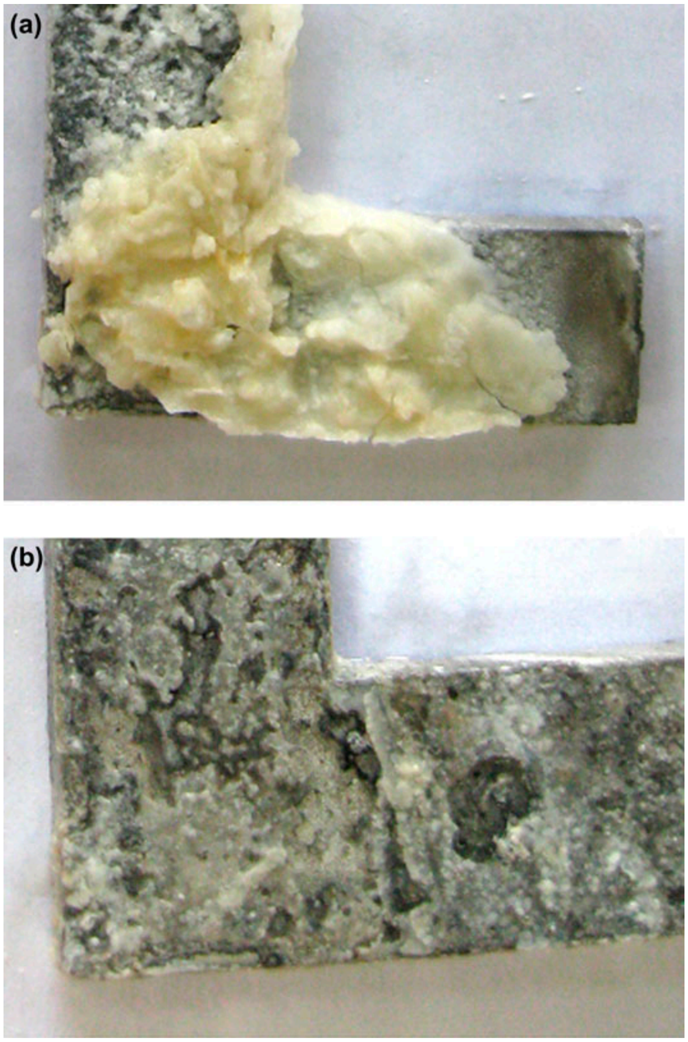

Fig. 14. The features of electrode surface: (a) anode surface; (b) cathode surface.

Table 5
Regression coefficients, and corresponding F and p values for effluent silica concentration

Factor	Coefficient estimate	Sum of squares	df	Mean square	F value	p-value Prob > F
Intercept	10.58	–	1	–	–	–
x_1	−8.78	154.22	1	154.22	146.07	<0.0001
x_2	−1.96	7.69	1	7.69	7.28	0.0428
x_3	−10.66	227.14	1	227.14	215.13	<0.0001
$x_1\ x_2$	−1.17	1.82	1	1.82	1.72	0.2464
$x_1\ x_3$	1.75	4.07	1	4.07	3.86	0.1067
$x_2\ x_3$	−1.95	5.08	1	5.08	4.81	0.0797
x_1^2	2.47	15.96	1	15.96	15.12	0.0115
x_2^2	0.32	0.27	1	0.27	0.26	0.6337
x_3^2	1.17	3.61	1	3.61	3.42	0.1237

Table 6
ANOVA results of the model for effluent silica concentration

Source	Sum of squares	df	Mean square	F value	p-value Prob > F
Model	1,031.12	9	114.57	108.51	<0.0001
Residual	5.28	5	1.06		
Lack of fit	5.28	1	5.28		
Pure error	0.000	4	0.000		

Notes: R^2 = 0.9949, adjR^2 = 0.9857, CV = 8.45%, AP = 39.901.

longer retention time means more contacting time to ensure more alum floc removing the certain silica content. Higher pH value of solution provides more OH^- to incorporate into $Al(OH)_{3(s)}$, which is the dominating monomer to remove silica. It can be seen from

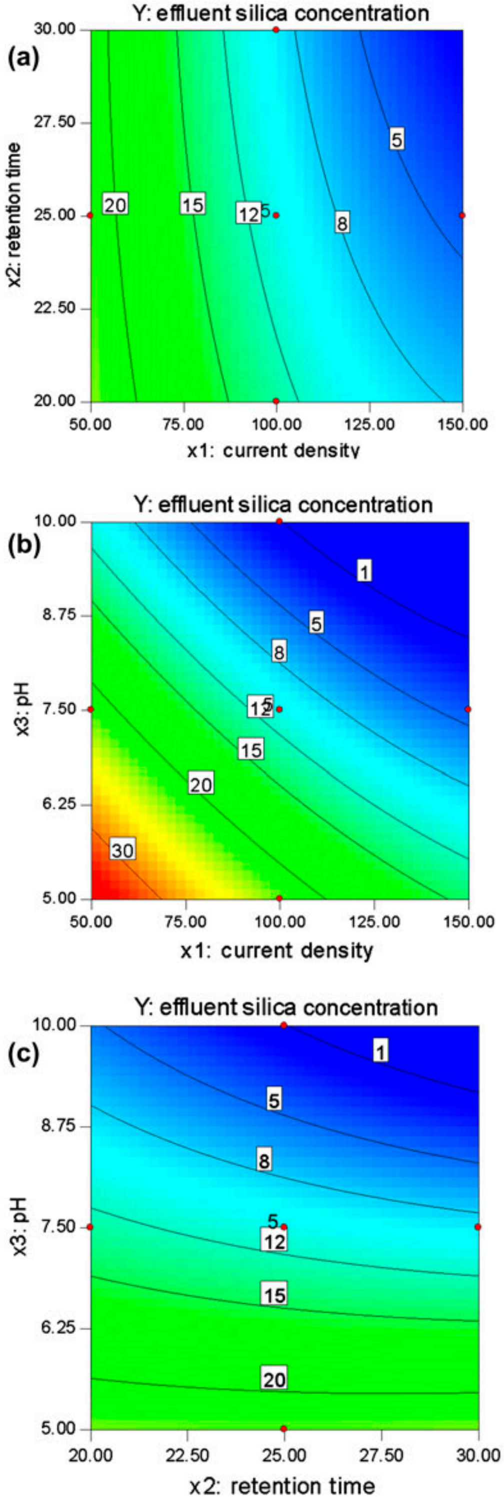

Fig. 15. Contour plots for the effect of (a) current density (A/m^2) and retention time (s); (b) current density (A/m^2) and pH; (c) retention time (s) and pH on effluent silica concentration (mg/L).

Fig. 15(a), a region below 5 mg/L can be obtained when current density is higher than 125 A/m^2 and the retention time longer than 24 s. A region below 2 mg/L can be obtained when current density is higher than 145 A/m^2 and the retention time longer than 29 s. A region below 5 mg/L can be obtained when current density is higher than 75 A/m^2 and the pH value higher than 7.4, from Fig. 15(b). And the same region was gained when the retention time was longer than 20.5 s and the pH value was higher than 8.65, from Fig. 15(c).

The Design-Expert software can be used to optimize the experimental results, on the basis of the operator's requirements to achieve different project purposes [35]. Here, effluent silica concentration is targeted at 5 mg/L. The optimum condition was current density 144.06 A/m^2, retention time 25.95 s, and pH value 7.29, which gave an effluent silica concentration below 5 mg/L.

4. Conclusions

The paper aims at studying the effects of various ions on the behavior of aluminum electrode in a continuous electrocoagulation system for silica removal. It was found that the anodic overpotential runs the whole applied voltage due to the passivation on the anode surface. These types of anions have different effects on the voltage rise. After comparing the interaction of different anions on the electrode behavior, the solution with $[NO_3^-]/[SO_4^{2-}] = 0.1$ is the most favorable supporting electrolyte in electrocoagulation process for silica removal. A second-order polynomial equation is obtained to predict the silica removal. The optimization of silica removal process was investigated using RSM. This work provides guiding significance for the practical application of electrocoagulation process.

References

[1] K.D. Demadis, E. Mavredaki, Green additives to enhance silica dissolution during water treatment, Environ. Chem. Lett. 3 (2005) 127–131.

[2] C.H. Koo, A.W. Mohammad, F. Suja, Recycling of oleochemical wastewater for boiler feed water using reverse osmosis membranes—A case study, Desalination 271 (2011) 178–186.

[3] Y.D. Pan, F.Q. Si, Z.G. Xu, C.E. Romero, An integrated theoretical fouling model for convective heating surfaces in coal-fired boilers, Powder Technol. 210 (2011) 150–156.

[4] Y. Zeng, C.Z. Yang, W.H. Pu, X.L. Zhang, Removal of silica from heavy oil wastewater to be reused in a boiler by combining magnesium and zinc compounds with coagulation, Desalination 216 (2007) 147–159.

[5] Z.H. Liang, S. Li, W.Q. Guo, C.M. Fan, The kinetics for electrochemical removal of ammonia in coking wastewater, Chin. J. Chem. Eng. 19 (2011) 570–574.

[6] M.S. Secula, L. Zaleschi, C.S. Stan, I. Mămăligă, Effects of electric current type and electrode configuration on the removal of Indigo Carmine from aqueous solutions by electrocoagulation in a batch reactor, Desalin. Water Treat. (2013) 1–10.

[7] S.L. Gelover-Santiago, S. Pérez-Castrejón, A. Martín-Domínguez, I.E. Villegas-Mendoza, Electrogeneration of aluminium to remove silica in water, Water Sci. Technol. 65 (2012) 434–439.

[8] Z. Liao, Z. Gu, M.C. Schulz, J.R. Davis, J.C. Baygents, J. Farrell, Treatment of cooling tower blowdown water containing silica, calcium and magnesium by electrocoagulation, Water Sci. Technol. 60 (2012) 2345–2352.

[9] M.C. Schulz, J.C. Baygents, J. Farrell, Laboratory and pilot testing of electrocoagulation for removing scale-forming species from industrial process waters, Int. J. Environ. Sci. Technol. 6 (2009) 521–526.

[10] W. Den, C.J. Wang, Removal of silica from brackish water by electrocoagulation pretreatment to prevent fouling of reverse osmosis membranes, Sep. Purif. Technol. 59 (2008) 318–325.

[11] C.T. Wang, W.L. Chou, L.S. Chen, S.Y. Chang, Silica particles settling characteristics and removal performances of oxide chemical mechanical polishing wastewater treated by electrocoagulation technology, J. Hazard. Mater. 161 (2009) 344–350.

[12] W. Den, C.P. Huang, Electrocoagulation of silica nanoparticles in wafer polishing wastewater by a multichannel flow reactor: A kinetic study, J. Environ. Eng. 132 (2006) 1651–1658.

[13] W. Den, C.P. Huang, H.C. Ke, Mechanistic study on the continuous flow electrocoagulation of silica nanoparticles from polishing wastewater, Ind. Eng. Chem. Res. 45 (2006) 3644–3651.

[14] W. Den, C.P. Huang, Electrocoagulation for removal of silica nano-particles from chemical-mechanical-planarization wastewater, Colloids Surf., A 254 (2005) 81–89.

[15] M. Mechelhoff, G.H. Kelsall, N.J.D. Graham, Electrochemical behaviour of aluminium in electrocoagulation processes, Chem. Eng. Sci. 95 (2013) 301–312.

[16] J.L. Trompette, H. Vergnes, On the crucial influence of some supporting electrolytes during electrocoagulation in the presence of aluminum electrodes, J. Hazard. Mater. 163 (2009) 1282–1288.

[17] G. Mouedhen, M. Feki, M.D.P. Wery, H.F. Ayedi, Behavior of aluminum electrodes in electrocoagulation process, J. Hazard. Mater. 150 (2008) 124–135.

[18] A.R. Amani-Ghadim, S. Aber, A. Olad, H. Ashassi-Sorkhabi, Influence of anions on Reactive Red 43 removal in electrochemical coagulation process, Electrochim. Acta 56 (2011) 1373–1380.

[19] D. Ghernaout, B. Ghernaout, On the controversial effect of sodium sulphate as supporting electrolyte on electrocoagulation process: A review, Desalin. Water Treat. 27 (2011) 243–254.

[20] M. Behbahani, M.R.A. Moghaddam, M. Arami, Techno-economical evaluation of fluoride removal by electrocoagulation process: Optimization through response surface methodology, Desalination 271 (2011) 209–218.

[21] F. Akbal, S. Camcı, Comparison of electrocoagulation and chemical coagulation for heavy metal removal, Chem. Eng. Technol. 33 (2010) 1655–1664.

[22] C. Exley, J.D. Birchall, A mechanism of hydroxyaluminosilicate formation, Polyhedron 12 (1993) 1007–1017.

[23] T.H. Nguyen, R.T. Foley, The chemical nature of aluminum corrosion, J. Electrochem. Soc. 129 (1982) 27–32.

[24] C.Y. Hu, S.L. Lo, W.H. Kuan, Effects of co-existing anions on fluoride removal in electrocoagulation (EC) process using aluminum electrodes, Water Res. 37 (2003) 4513–4523.

[25] J. Bernard, M. Chatenet, F. Dalard, Understanding aluminum behaviour in aqueous alkaline solution using coupled techniques, Electrochim. Acta 52 (2006) 86–93.

[26] Y.S. Yıldız, A.S. Koparal, B. Keskinler, Effect of initial pH and supporting electrolyte on the treatment of water containing high concentration of humic substances by electrocoagulation, Chem. Eng. J. 138 (2008) 63–72.

[27] L.F. Lin, C.Y. Chao, D.D. Macdonald, A point defect model for anodic passive films, J. Electrochem. Soc. 128 (1981) 1194–1198.

[28] R. Ambat, E.S. Dwarakadasa, Studies on the influence of chloride ion and pH on the electrochemical behaviour of aluminium alloys 8090 and 2014, J. Appl. Electrochem. 24 (1994) 911–916.

[29] S.I. Pyun, E.J. Lee, Effect of halide ion and applied potential on repassivation behaviour of Al-1 wt.% Si-0.5 wt.% Cu alloy, Electrochim. Acta 40 (1995) 1963–1970.

[30] W.J. Lee, S.I. Pyun, Effects of sulphate ion additives on the pitting corrosion of pure aluminium in 0.01 M NaCl solution, Electrochim. Acta 45 (2000) 1901–1910.

[31] R.T. Foley, T.H. Nguyen, The chemical nature of aluminum corrosion, J. Electrochem. Soc. 129 (1982) 464–467.

[32] N. Daneshvar, H. Ashassi-Sorkhabi, A. Tizpar, Decolorization of orange II by electrocoagulation method, Sep. Purif. Technol. 31 (2003) 153–162.

[33] T. Harif, M. Khai, A. Adin, Electrocoagulation versus chemical coagulation: Coagulation/flocculation mechanisms and resulting floc characteristics, Water Res. 46 (2012) 3177–3188.

[34] M. Amini, H. Younesi, N. Bahramifar, A.A.Z. Lorestani, F. Ghorbani, A. Daneshi, M. Sharifzadeh, Application of response surface methodology for optimization of lead biosorption in an aqueous solution by *Aspergillus niger*, J. Hazard. Mater. 154 (2008) 694–702.

[35] M.S. Secula, I. Cretescu, B. Cagnon, L.R. Manea, C.S. Stan, I.G. Breaban, Fractional factorial design study on the performance of GAC-enhanced electrocoagulation process involved in color removal from dye solutions, Materials 6 (2013) 2723–2746.